Microwave Review
December 2024, Vol. 30, No. 2, pp. 3-14
DOI: 10.18485/mtts_mr.2024.30.2.1

Compressed Sensing Image Communication in Rayleigh Fading Channel Using Polar Code

Arti Kumari and Sanjeet Kumar

Abstract – **In modern wireless communication systems, the efficient transmission of high-quality images is a matter of paramount importance. In recent several years, *compressed sensing* (CS) has emerged as a powerful technique for reducing the energy consumption, improving the data compression, and lowering the bandwidth requirements for an image transmission. However, communication channels, especially wireless channels, often introduce various forms of interferences and fading, such as Rayleigh fading, which can severely degrade the received image quality. This paper proposes a novel approach that combines compressed sensing with polar code to improve the reliability of image communication through a Rayleigh fading channel. In this work first, we leverage the advantages of compressed sensing to significantly reduce the amount of data that needs to be transmitted while maintaining acceptable image quality. By exploiting sparsity of the standard images, we can sample and compress the images efficiently. Next, we have applied polar code, known for its superior error correction capabilities, to protect the compressed data from channel induced errors. The paper presents a comprehensive evaluation of the proposed system, including theoretical performance bounds and simulations in a Rayleigh fading channel. Our results demonstrate that the combination of compressed sensing and polar coding outperforms traditional communication schemes in terms of both optimal bandwidth requirement and image quality in the form of its reliability under challenging fading environments. This approach offers a promising solution for efficient and robust image transmission over wireless channels, with applications in remote sensing, surveillance, medical imaging, and many more. This paper focuses on choosing an optimum error correction scheme tailored for compressed sensing signals under severe channel conditions. The performance of the reconstructed image has been evaluated based on the performance parameters such as *peak signal-to-noise ratio* (PSNR), *structural similarity* (SSIM) index and *bit error rate* (BER) under multipath fading conditions. Simulation results show the superior performance of the proposed model at a very low *signal-noise ratio (*SNR) in the range of 2.5 to 3.6 dB.**

Keywords – **Compressed sensing, image communication, Rayleigh fading channel, polar code, wireless communication, error correction, image quality.**

Article history: Received January 24, 2024; Accepted April 30, 2024

Arti Kumari and Sanjeet Kumar are with the Electronics and Communication Engineering, Birla Institute of Technology, Mesra, Ranchi, 835215, Jharkhand, India,

E-mails: phdec10004.20@bitmesra.ac.in, sanjeet@bitmesra.ac.in

I. INTRODUCTION

In the realm of Modern wireless communication, the transmission of high-quality images has become increasingly essential for a multitude of applications, spanning from remote surveillance and medical imaging to multimedia content delivery. However, the inherently limited bandwidth of wireless channels poses a significant challenge to the efficient transmission of images, especially in the presence of adverse channel conditions such as Rayleigh fading. *Compressed Sensing* (CS) has emerged as a powerful technique to mitigate these challenges by significantly reducing the amount of data required for image transmission. Additionally, Polar Codes have gained recognition for their remarkable error correction capabilities. This paper explores the fusion of two innovative concepts CS and Polar Code to address the problem of image communication in a Rayleigh fading channel. In wireless communication [1-3], images are typically transmitted as large datasets, demanding substantial bandwidth resources. It results not only inefficient spectrum utilization but also makes image transmission vulnerable to channel impairments, including multi-path fading. Rayleigh fading, a characteristic of wireless channels, introduces random amplitude and phase variations to the transmitted signal, which can severely degrade the image quality. Therefore, there is a pressing need for novel techniques that can enable efficient image transmission, even in challenging fading environments. CS has gained prominence as an indigenous solution to this bandwidth bottleneck. It exploits the inherent sparsity of test images, wherein only a small fraction of the image's coefficients carries significant information. By strategically sampling and compressing these coefficients, CS allows for the reconstruction of the original image with high fidelity. The compression technique not only conserves bandwidth but also enhances the resilience of image transmission in adverse channel conditions [4–6]. Polar Codes, on the other hand, have raised to prominence for their superior error correction capabilities. These codes, pioneered by Arikan, have been adopted in various communication standards due to their capacity-achieving properties. It effectively corrects the errors induced by the channel, making them a potent tool for enhancing communication reliability [9, 12]. The primary objective of this research is to leverage the strengths of Compressed Sensing and Polar Coding to address the challenges posed by image communication in a Rayleigh fading channel. By integrating CS for bandwidth-efficient image compression and Polar Codes for robust error correction [13, 15], we aim to achieve high-quality image transmission even in scenarios characterized by significant channel fading. In the subsequent sections of this paper, we will delve into the technical details of our proposed approach,

conduct theoretical analyses, and present simulation results to demonstrate the advantages of this fusion of Compressed Sensing and Polar Coding. The findings of this research hold the potential to revolutionize image communication in wireless networks, enabling efficient and reliable transmission of images over Rayleigh fading channels for a wide range of applications. Although, CS is a lossy data compression technique. However, it has been applied in various applications [16] and solved several practical challenges in recent years. The performance of compressive sensing with the data transmission over the wireless network, data acquisition, and data reconstruction method for images is evaluated and analysed in this research work. Nowadays, the increasing demand for internet services for various applications in daily life also poses critical challenges regarding the storage of huge visual data apart from its reliable communication through fading channels. However, in digital television broadcasting, the time latency between the data arriving at the receiver and the delivered image data on the TV screen is set in one directional transmission. However, this is not considered a critical issue because the old Analog TV receivers have this capability [17]. However, time latency becomes a critical issue in a live exchange of medical images and mobile phone conversations in two-directional digital communication systems. Errors and low efficiency may be induced during communication. The low efficiency and the high latency in modern digital communication are the general challenges faced during communication [18, 19]. The compressed sensing-speech coding scheme is utilized for mobile communications in [20] but it is more complicated even for speech signals. In [21], an efficient compressed image transmission scheme has been proposed for wireless networks based on *orthogonal frequency division multiplexing* (OFDM). However, this paper used the block compressed sensing method, which involves: block sparse chaotic DCT basis matrix and block chaotic DCT measurement matrix. In [16, 17], an efficient compressed image transmission scheme has been proposed for wireless networks based on OFDM which involves: a Hadamard sparse basis matrix partial DCT measurement matrix and 16-QAM-OFDM system with *visible light communication* (VLC) channel. A Gaussian random measurement matrix with a QAM-OFDM transmission system has been used in for efficient image transmission using CS. Therefore, we used error correction codes such as polar code [9] that give better performance. Polar code was recently used in 5G mobile phone systems [11, 13] to increase efficiency and reduce the latency during communication [13].In this manuscript, we have demonstrated that utilizing polar codes with *successive cancellation* (SC) decoding outperforms traditional error-correcting codes in the context of image communication. The primary objective of this paper is to assess the fidelity of grayscale images transmitted through a communication system. In this system, grayscale images are encoded using Polar codes and then transmitted over a multipath channel using OFDM modulation and SC decoding. This evaluation is conducted across a range of signal-to-noise ratio (E_b/N_0) values from 0 dB to 5 dB, which correspond to low signal-to-noise ratios. This investigation is particularly significant as prior literature has not previously explored the performance of SC decoding at low signal-to-noise ratios in the context of image transmission with Polar codes. Recently, compressive sensing schemes have been used for the fifth-generation system to handle the huge amount of generated data. Also, it gives better reliability for the reconstructed data. The aim of this paper is to be encoded by polar code for error correction of the compressed data before communication.

Our contributions to this study are summarized as follows:

- The primary objective of this research is to leverage the strengths of Compressed Sensing and Polar Coding to address the challenges posed by image communication in a Rayleigh fading channel. By integrating CS for bandwidth-efficient image compression and Polar Codes for robust error correction, we aim to achieve high-quality image transmission even in scenarios characterized by significant channel fading.
- Performance evaluation of Polar code for reliable transmission of compressed sensing images.
- Transmission of a gray image encoded with polar code and decoded with successive *cancellation* (SC) decoder in the presence of a multipath fading channel.
- Proposed a *Compressive Sensing–Polar Code–OFDM* (CS-PC-OFDM) system model to improve the efficient and reliable communication of compressed image data.

The following sections of this paper are organized in the following manner: Section II briefly covers compressed sensing and polar codes, including a mention of SC decoding and the methodology used in this investigation. Sections III, IV and V present Performance Parameters, results and conclusions, respectively.

I. Backgrounds of Compressed Sensing and Polar Code

A. Compressed Sensing

Compressive sensing is a signal-processing scheme developed in 2006[1]. It reconstructs the sparse signal from a small set of linear measurements using a proper transform [18]. Let us consider a sparse signal in a time domain ψ with size $N\times1$. The sparse signal, x can be expressed in terms of original signal, X as follows:

$$x = \psi \times X \,, \tag{1}$$

where x is considered to be a Kth order sparse signal with size $N\times N$ if there are K ($K \ll M$) nonzero elements in x. Suppose y is a measurement array with ($M \ll N$) and can be expressed as

$$y = \phi \times x \,, \tag{2}$$

where ϕ is a measurement matrix of size $M\times N$. The measurement matrix ϕ can be constructed using a chaotic map, random Gaussian matrix, Bernoulli matrix, etc. In this paper, we have used Teoplitz diagonal measurement metrics to measure the signal. The perfect recovery of x from y requires two matrices ϕ and ψ to obey (a) the incoherence condition and (b) the restricted isometry property. Teoplitz diagonal measurement matrix satisfy these two conditions. In

this work, we have used the conventional *orthogonal matching pursuit* (OMP) algorithm for efficient and reliable reconstruction of the signal. The proposed *Teoplitz diagonal measurement matrix* (TDM) is based on the Toeplitz matrix that only keeps the entities in a diagonal line set as '1'. The construction of TDM is exposed with equation (3).

$$\phi_{i,j} = \begin{cases} 1, & \\ 1, & \text{for } i = 1 \text{ or } j = 1 \text{ or } i = j \\ 0, & \text{Otherwise} \end{cases}, \quad (3)$$

where $\phi_{i,j} \in R^{M \times N}$, $i \in (1, M)$, $j \in (1, N)$. This is the proposed TDM measurement matrix.

$$\phi_{M \times N} = \begin{bmatrix} 1\,0\,0\,0 \cdots 0 \\ 0\,1\,0\,0 \cdots 0 \\ \cdot\ \cdot\ \cdot\ \cdot\ \cdot\ \cdot \\ \cdot\ \cdot\ \cdot\ \cdot\ \cdot\ \cdot \\ \cdot\ \cdot\ \cdot\ \cdot\ \cdot\ \cdot \\ 0\,0\,0\,0 \cdots 0 \end{bmatrix}$$

Algorithm1: Modified Compressive Sensing based on Toeplitz Diagonal Measurement Matrix

Input: *Input Signal measurement ϕ of Matrix size $M \times N$ ($M << N$)*
Output: *Recovered sparse signal x'*
1. Initialize:
   -Set iteration count i = 1
   -Set measurement y as an empty array
2. Sparse representation
   a.Generate sparse signal using DWT basis transform:
   b.Compute measurement y:
   -Multiply the sensing matrix ϕ by the signal x: $y = \phi.x$
   c.Update the measurement y:
   -Concatenate the measurement y_i to the existing measurement y
   d.Increment the iteration count i=i+1
3. Perform sparse recovery:
   a.Solve the optimization problem to recover the sparse signal x':
   -Minimize x' subject to $y = \phi.x'$
   b.Obtain the recovered sparse signal x'

B. Polar Code

In this section, the encoding and decoding process of polar code has been explained over the multi-path fading channel.

B.1 Encoding

The encoding process includes the redundant indices selection, assigning frozen bits to those redundancies according to worst-to-best channel condition, and then performing a polar transform on those bits. Now, a kernel for the polar transform is considered as shown in Figure 1.

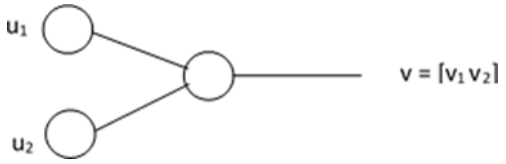

Fig. 1. Binary tree representation of a 2x2 kernel of polar transform

Here the input is $\mathbf{u} = [u_1 u_2]$ and the polar transform out- put is $\mathbf{v} = [v_1 v_2]$. This is sent through a multipath fading channel. Where v_1 and v_2 are equal to $u_1 \oplus u_2$ and u_2 respectively. So the binary tree for a polar code having $N = 8$ will look like the diagram given next. The binary tree is used for encoding and decoding an (8,4) polar code as shown in Figure 2, where the coded block length, N is 8 and the data block length, K is 4. The darkened nodes show the frozen positions where the redundant bits are added. It can be seen that the tree has $\log_2(N) + 1$ depth. It saves the last depth or the leaf nodes and at every depth the modulo addition is carried out on N bits while encoding. The complexity order can be expressed as $O(N\log_2 N)$. Encoding starts at the last depth of the tree. During the decoding, the vector received after demodulation is supplied to the topmost node of the tree after which they are sliced into half at every successive node and then processed till the last leaf node is reached where the decision is taken based on a single bit. The details of the polar code and successive cancellation decoding have been discussed in the following section.

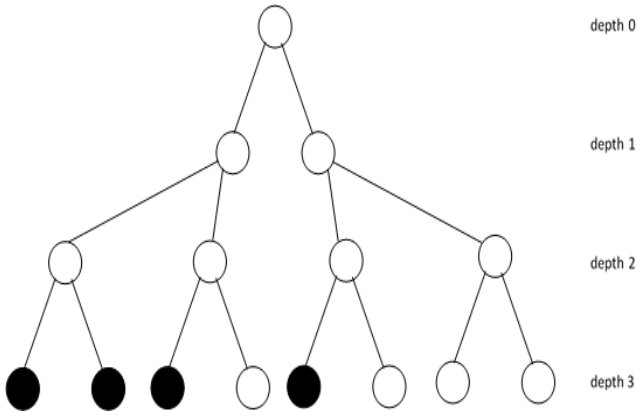

Fig. 2. Binary tree for $N = 8$, $K = 4$

B.1.1 Polar Encoding

The encoding process begins by selecting the redundant indices, assigning frozen bits to those redundancies, and applying a polar transform to those bits. Let K denote the number of data bits to be encoded. The data vector is denoted by $u_{1\times K} = [u_1 u_2 \ldots\ldots u_K]$. Initially, we determine the block length N based on the desired code rate (K/N). Subsequently, a reliability sequence is generated for N split channels, organised from worst to best reliability indices. Upon generating the sequence, the first (N-K) indices mentioned in

the reliability sequence are designated as frozen positions. These indices are then populated with fixed or dynamically generated frozen symbols. In this case, we've chosen the frozen symbols to be fixed, namely 0. Let the resulting vector be represented as:

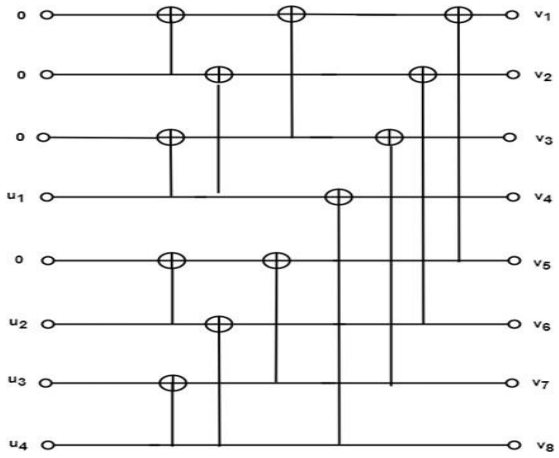

Fig. 3. A N = 8, K = 4 polar encoder where the frozen positions are given by F = (1, 2, 3, 5)

$c_{1\times N}$ = [0 0 0 u_1 0 u_2.....u_K The elements of this vector undergo iterative channel recombination multiple times, as described previously. This process can be essentially summarised by the expression: $V = cG_2^{\oplus n}$ as mentioned in the previous sections. It is to be noted that v is of the same size (1×*N)* as c. The vector v is then modulated with *binary phase shift keying* (BPSK) modulation and transmitted over the channel. In Figure 3 we see the example where the 2×2 kernel has been used as the elementary node for constructing the (8, 4) polar code encoder structure. Here u_i, where *i (*1, *K*), are the data bits. The frozen bits are set to 0 here and the indices correspond to the 4 split channels with the lowest capacities. If two channels have the same capacity they are indexed in their natural order.

B.2. Successive Cancellation Decoding for Polar Codes

The decoding of polar codes follows the ideology behind the *single parity check* (SPC) code and the *soft-in-soft-out* (SISO) decoder. In the SPC encoder, the parity bit is set by taking the XOR of all the input bits. The SISO decoder decodes this code by calculating by log –the likelihood ratios (LLRs) of the code alphabets concerning the received data from the channel. Using this basic principle, Arikan proposed the SC decoder to decode polar codes [9]. It operates sequentially, i.e., the first bit is decoded with the received values from the channel while the subsequent bits are decoded with both the information received from the channel and the decisions taken about the previous bits. It treats every subsequent bit like a parity bit generated from the previous bits, following the concept of channel splitting. In addition to this, the decoder has the knowledge of the frozen indices, so the errors occurring while decoding the frozen bits are caught and then used to cancel out the errors occurring during the decoding of the other bits, hence its name, successive cancellation. In this section we will see the performance of the SC decoder, the addition of list decoding via a CRC check to the SC decoder proposed by Tal and Vardi in [11], and the resulting improvement over the SC decoder offered by this modification. We've employed the simplified binary tree method for developing the SC decoding algorithm. The received channel values are first converted to channel beliefs by:

$$L_i = \frac{2y_i}{\sigma^2}. \tag{4}$$

This vector **l**= [l_1 l_2 l_3.... l_N] is subsequently fed as input to the uppermost node. This vector is then split in half, yielding a_l and b_l, each with sizes of 1×*N*/2. Next, a bitwise operation is conducted on these vectors.

$$f\left(a_i, b_i\right) = \frac{a_i, b_i}{|a_i|, |b_i|}\left(min\left(|a_i|, |b_i|\right)\right). \tag{5}$$

The resultant 1×*N*/2 sized vector is subsequently transmitted to the right child. This procedure of splitting and executing operation (6) is reiterated until reaching the terminal node of the tree, where the sizes of vector a_l and b_l become 1×1. At this leaf node, the estimation of the bit u_i is computed according to the sign of the LLR *(Log-Likelihood Ratio*) value received from the parent node.

$$f\left(x\right) = \begin{cases} 0, & \text{for } i \in f \\ 1, & \text{for } a_i < 0 \\ 0, & \text{for } a_i \geq 0 \end{cases} \tag{6}$$

Afterward, f represents the sequence of frozen indices. Upon completion, the decision made by the node is passed to its parent node. This parent node conducts LLR calculation using:

$$g\left(a_i, b_i\right) = b_i + \left(1 - 2\hat{u}_i\right)a_i. \tag{7}$$

This calculated value is subsequently sent to the left child of the node. If the left child is a leaf node, it decides on the bit based on the sign of the calculated value, denoted as $\hat{u}_2$, in the equation (5). This decision is then relayed to the parent node, which executes a polar transform on $\hat{u}_1$ and $\hat{u}_2$ and forwards the decision to its parent node. This recursive process continues until the decoding of the very last bit. These functions are simplified approximate forms of the rigorous probability domain calculation of LLRs based on the conditional probability of the alphabet symbols, given the channel outputs and the previously decoded bits. This simplification is possible due to the binary nature of the code symbols. Figure 4 is the diagrammatic representation of a 2×2 kernel of the SC decoder in simplified binary tree form. From equation (6) LLR-based *Binary Phase Shift Keying* (BPSK) decoding utilizes *Log-Likelihood Ratios* (LLRs) to make decisions about the transmitted bits. In BPSK, each transmitted bit is represented by a specific phase of the carrier signal. During decoding, the receiver needs to determine which bit was sent based on the received signal. The LLR is a measure of how likely it is that a particular bit was transmitted, given the received signal. In LLR-based

decoding, the LLR value associated with each bit position (index) is calculated based on the received signal and the known properties of the modulation scheme. The ith index (a_i) refers to the LLR associated with the ith bit position. This value is used in the decoding process to determine the most likely bit value for that position. Since the LLR values are calculated based on the received signal, the decoding process inherently depends on the characteristics of the received data. Different received signals will result in different LLR values, leading to potentially different decisions about the transmitted bits. Therefore, LLR-based BPSK decoding adapts to variations in the received data, making it dependent on the specific data being received.

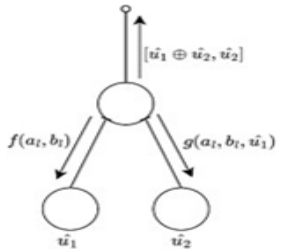

Fig. 4. 2x2 kernel of the successive cancellation decoder showing the node functions and the directions in which the decisions of the node operations are sent

B3. CS-PC-OFDM Model

In this section, we have proposed the Compressive Sensing–Polar Code–OFDM (CS-PC-OFDM) system model to improve the efficient and reliable communication of compressed image data. In communication, data suffer from *inter-symbol interference (*ISI) and signal attenuation due to the multi-path fading channel. In this manuscript, the multi-path fading channel is used which has several signal paths. The multi-path fading channel is recognized as the worst channel [23, 24]. Here the signal power changes by the Rayleigh distribution. It works best in situations where, there is no dominant signal (direct line of sight signal). To reduce the channel impact, proper channel compensation schemes are chosen. So, a detailed block diagram of compressed image communication using a polar-coded CS- OFDM model is shown in Figure 6. This model allows us to perform signal acquisition and compression to reduce networks loading by using CS *Compressive Sensing* with polar code in wireless networks simultaneously.

The proposed model consists of compressive sensing as a source coding, polar code as a channel encoding, and *orthogonal frequency division multiplexing* (OFDM)as a modulator. Polar code is a network encoding method used to reduce the transmission error rate. It works by adding extra digits to information that is transmitted to enable error detection and correction by the recipient. A polar encode with a code rate of K/N has N output bits and K input bits. The successive cancellation decoder is used to decode the polar codes. *Inter symbol interference* (ISI) and signal attenuation are the major problems for signal communications through multipath channels [25–27]. To overcome these effects the OFDM is used. It is a multicarrier modulation technique used in several OFDM (CS-PC- OFDM) system models to improve the efficient and reliable communication of compressed image data. In communication, data suffer from *inter-symbol interference* (ISI) and signal attenuation due to the multi-path fading channel. In this manuscript, the multi-path fading channel is used which has several signal paths. The multi-path fading channel is recognized as the worst channel [28]. Here the signal power changes by the Rayleigh distribution. It works best in situations where there is no dominant signal (direct line of sight signal). To reduce the channel impact, proper channel compensation schemes are chosen. So, a detailed block diagram of compressed image communication using a polar-coded CS- OFDM model is shown in Figure 6. This model allows us to perform signal acquisition and compression to reduce network loading by using CS *Compressive Sensing* with polar code in wireless networks simultaneously. The proposed model consists of compressive sensing as a source coding, polar code as a channel encoding, and *orthogonal* communication standards to avoid the impact of multipath fading and to ensure reliable communication at high data rates [21]. It improves the results by using different weighting factors depending on *signal-to-noise ratios* (SNR). The inverse operations are performed in OFDM demodulation as it is used in the transmission side.

TABLE 1
SIMULATION PARAMETER

S.No	Parameter	Details
1.	Input image	Lena, Barbara, Boat, peppers, and Cameraman
2.	Sparse basis Transform	DWT
3.	Measurement matrix	Toeplitz Diagonal measurement
4.	Polar code parameter	(8, 4) and (1024, 512)
5.	Channel coding	1/2 polar code
6.	Channel decoding	SC decoding
7.	Channel mode	Rayleigh fading channel
8.	Number of paths nTaps	3
9.	Reconstruction method	Orthogonal Matching Pursuit

Successive cancellation decoding and the orthogonal matching pursuit are used to reconstruct the signal at the receiver side. Table 1 presents the simulation parameters used during the simulation.

C. Communication System Description

A block diagram for the proposed model has been shown in Fig. 5. The system parameters used in the CS-PC-OFDM model are tabulated in Table 1. Currently, five different types of input images of size 256×256 have been taken for multipath propagation. These images are Lena, Boats, Peppers, and Cameraman. To begin, these images undergo compression through a compressed Sensing scheme.

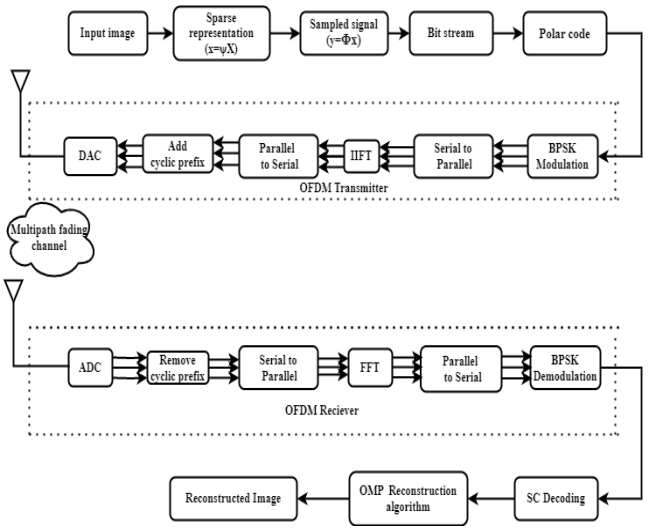

Fig. 5. Block diagram of compressed image communication using a polar-coded CS-OFDM system

Subsequently, the compressed data is subjected to polar encoding before being processed through an OFDM modulator and transmitted across a multipath fading channel. Upon reception, the images are subjected to an OFDM demodulator before decoding via the respective SC decoder. The quality of the reconstructed images is then assessed using four distinct image quality evaluation metrics: peak signal-to-noise ratio, NPCR, UACI, and structural similarity (SSIM). PSNR, NPCR, and UACI evaluate the discrepancy in luminance values between corresponding pixel coefficients in the original and reconstructed images, providing an indication of image quality. However, it's important to note that PSNR is not considered a metric that aligns with human visual perception [21]. Therefore, another metric, SSIM, which relies on the structural vector components of the image, is also employed. These additional metric accounts for the visual quality of the received image. This comprehensive approach enables a more meaningful investigation of image transmission. The formulas for PSNR, NPCR, UACI, and SSIM are given by equations 10, 11, 12, and 13, respectively.

II. PERFORMANCE PARAMETER

A new design for signal coding based on the combination of CS and OFDM is proposed to be used in communications. It is integrated into an end-to-end communication system. The Following are the performance measures that are used in this paper.

Compression Ratio: In our work, the five test images Lena, Barbara, Boat, peppers, and Cameraman images are used. The test image is first converted into a sparse signal on a DWT sparse basis. The obtained sparse signal is measured by a Toeplitz-Diagonal measurement matrix. Then encoded by polar code and then transmitted to the channel. And at the receiver, SC decoding is used to remove the error of the channel. A conventional OMP reconstruction algorithm is employed to reconstruct the signal. The simulation results are obtained using MATLAB. The compressive sensing schemes are performed based on the different *compression ratios* (CR). The compression ratio is defined [22–24] as

$$CR = \frac{M}{N}, \tag{8}$$

where M and N are the lengths of the observation vector and the input signal, respectively. From this formula, lower CR means higher compression.

Mean square error and Peak to signal noise ratio:

The Peak signal-to-noise ratio (PSNR) and mean square error (MSE) are defined as follows [14]:

$$MSE = \frac{1}{rc}\sum_{i=0}^{r-1}\sum_{j=0}^{c-1}\left[\left(X(i,j) - x(i,j)\right)\right]^2, \tag{9}$$

where *r* and *c* denote the image row and column, respectively. $X(i,j)$ and $x(i,j)$ show the gray values of the reconstructed and the original images, respectively. The high value of PSNR represents the better quality of the reconstructed image. The Peak Signal-to-Noise Ratio (PSNR) is defined as follows [14]:

$$PSNR(\text{dB}) = 10\log\frac{255^2}{MSE}. \tag{10}$$

NPCR and UACI: These parameters also aim to exploit the vulnerabilities in the reconstruction scheme by analysing the differences between two versions of the same image, typically an original image and a reconstructed image. It tries to deduce information about the reconstruction process by analysing the changes in the pixel values between the two images. It is called a differential attack. NPCR *(number of pixels change rate) and UACI (unified average changing intensity)* usually are used to examine the performance of resisting differential attack. NPCR and UACI are two commonly used parameters to measure the resistance of a reconstruction scheme against differential attacks. NPCR measures the percentage of pixels that differ between the original and reconstruction images. It provides an indication of the change introduced by the reconstruction process. The higher the NPCR value, the more effective the scheme is in altering the pixel values. A higher NPCR value, closer to 100%, indicates a higher level of pixel alteration and suggests a better resistance against differential attacks. UACI measures the average difference in intensity between corresponding pixels in the original and reconstruction images. It quantifies the average impact of the reconstruction process on the pixel values. UACI is typically reported as a value between 0 and 1. A lower UACI value suggests a smaller average change in pixel intensity and indicates a better resistance against differential attacks. NPCR and UACI are calculated as follows: Let us consider images $X(i, j)$ and $x(i, j)$, and their corresponding original images differ only by one pixel. Let $X(i, j)$ and $x(i, j)$ be the pixel values at the location (i, j) of *X* and *x*, respectively. Now, we construct a bipolar array D with elements 0 or 1 using the equation (11). The dimension of D is the same as the dimensions of *X* and *x*. The NPCR and UACI are computed by applying the following formulas.

$$D(i,j)=\begin{cases}1, \text{ if } X(i,j)\neq x(i,j)\\ 0, \text{ otherwise}\end{cases}, \quad (11)$$

$$NPCR=\frac{\sum_{i,j} D_{i,j}}{rc}, \quad (12)$$

$$UACI=\frac{1}{rc}\frac{\sum_{i,j}\left[\left(X(i,j)-x(i,j)\right)\right]}{255}. \quad (13)$$

Both NPCR and UACI provide quantitative measures to evaluate the effectiveness of reconstruction against differential attacks. Higher NPCR values and lower UACI values indicate stronger resistance to such attacks.

III. Result and Discussion

In this section, we illustrate some results of our proposed model to show the ability of the compressed sensing method and consequently its effect on the reconstruction process in wireless communication with multipath fading channels. The proposed model used a Rayleigh fading channel for transmitting the data but this is a worse-case scenario. After the compressive sensing source coding at the side of the transmitter, polar encoding is used to increase the robustness against channel induced errors and OFDM modulation is performed to enhance the efficiency and also the immunity against ISI caused by the channel. At the receiver side, the OFDM demodulation, followed by SC channel decoding is performed. In the beginning, we carried out an experiment by taking five test images, namely Cameramen, Lena, Barbara Boat, and Peppers for end-to-end communication with an error correcting polar code in the end-to-end transmission scheme for SNR=5dB. The reconstruction quality is measured by different parameters like *the Peak Signal to Noise Ratio* (PSNR), NPCR, MSE, and SSIM between the reconstructed image and the original image. The relative various performance analyses are present in this manuscript. We evaluate the system performance through subjective visualization of received images, along with measurements of bit error rate (BER) and PSNR. During simulation, the image in the sparse domain is sampled using *time-division multiplexing* (TDM) measurement matrices.

Orthogonal Matching Pursuit (OMP) algorithm is employed as the reconstruction method. Figure 6 depicts the reconstruction results of a different image, demonstrating the PSNR. Figure 6 show that Lena's reconstructed images get better performance than the others. And also shows a high compression ratio that is 0.4 we get a minimum PSNR of 28.1472dB with the Boat image and a maximum PSNR of 32.9285 dB with the Lena image. A higher PSNR value indicates a better reconstruction quality, as it implies a smaller amount of distortion or noise in the reconstructed signal. Figure 8 shows the comparison of *mean square error* (MSE) between five test images with the proposed errors correcting polar code with compressed sensing in the communications field. The proposed scheme achieves more accurate results in the reduction of MSE. Here, smaller values of MSE indicate a more accurate result and thus give a better quality of the reconstructed image. The *Number of Pixels Change rates (*NPCR) and the *Unified Average Changing Intensity* (UACI) were employed as a tool to judge the differences between images.

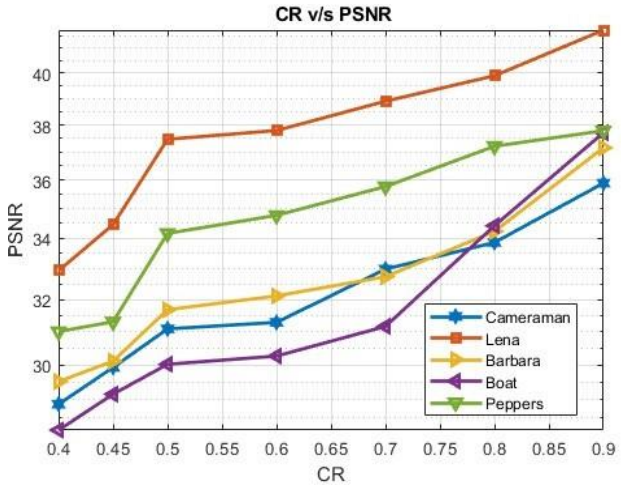

Fig. 6. Comparison of reconstruction performance (PSNR) versus different compression rates

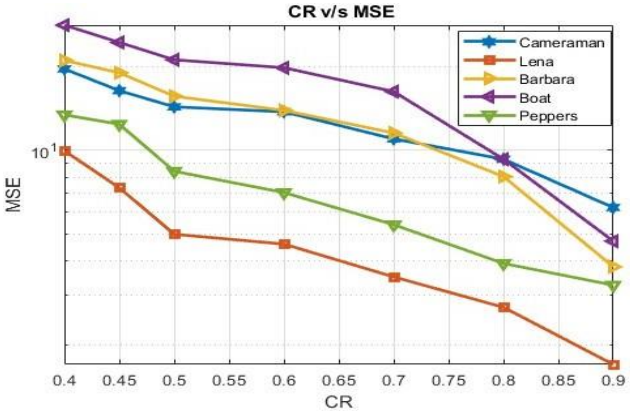

Fig. 7. Comparison of reconstruction MSE of different test images with different sampling rates

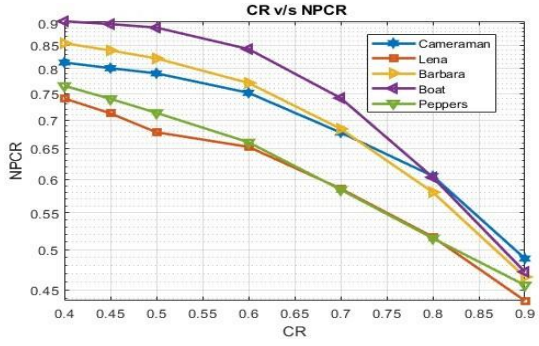

Fig. 8. Results of reconstruction NPCR of different test images with different sampling rates

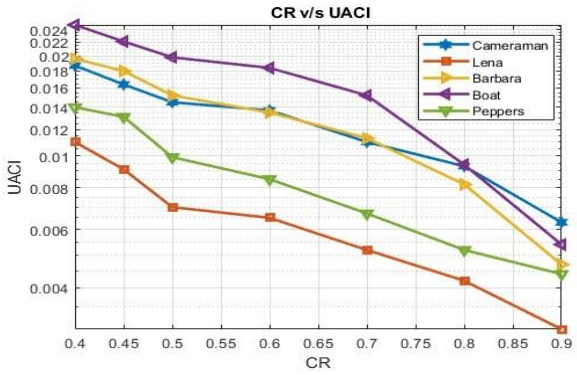

Fig. 9 Results of reconstruction UACI of different test images with different sampling rates

These two indicators are exploited to directly illustrate the changes between the reconstructed images and the test images. Figure 8 and Figure 9 show the NPCR and UACI results of the reconstructed images after communications, which decrease the NPCR and UACI values by decreasing the compression data rate. Figure 8 shows the NPCR results of the reconstructed images after communications. A higher NPCR value suggests that a larger percentage of pixels have changed between the original and reconstructed images. This indicates that the reconstruction process has introduced significant alterations to the pixel values, making it more challenging for an attacker to infer information about the original image from the reconstructed one. Therefore, if a higher NPCR value indicates better resistance against differential attacks, it means that the reconstruction algorithm is effectively altering a larger portion of the image, making it harder for attackers to exploit the differences between the original and reconstructed images to gather information about the reconstruction process. Figure 9 shows the UACI results of the reconstructed images after communications, which decrease UACI values by decreasing the compression data rate. And the reducing the compression data rate, the quality of the reconstructed images improves, as indicated by a decrease in UACI values. This aligns with the intuition that less aggressive compression preserves more image details, resulting in higher-quality reconstructed images. The performance of the polar code is shown in Fig. 10. The performance of the reconstructed image quality is good when the block length is increasing. The polar code with column weight two over GF (2) with N = 8 with K = 4 can maintain a better quality of the received image at a low SNR of 3.8dB. In this paper, image transmission is implemented using error-correcting polar code. The different standard images are tested as the original images, as shown in Fig. 10. PSNR of the proposed method can improve the performance of the received image at low SNR 3.8dB. Figure 11 shows the effects of different CR on SSIM values. The SSIM values are also decreasing with CRs, according to the results higher SSIM is consistent with a higher compression ratio. This figure also shows that the Lena image has better SSIM value performance (which should be 1 ideally) as compared to others. It means that our scheme also has very good compression recovery performance. We can see that the Boat image per form is the worst among the compared samples, more so at lower compression ratios.

TABLE 2

COMPARES THE PERFORMANCE OF DIFFERENT TEST IMAGES BASED ON CHANNEL AND WITHOUT CHANNEL. ALSO, IT COMPARES THE PERFORMANCE OF ERROR CORRECTING CODE BASED ON THE CONVOLUTION CODE AND POLAR CODE AT SNR =5dB AND CR=0.75

Image no	Image (256x256)	PSNR without channel error	PSNR with channel error but without channel coding	PSNR with Convolutional code	PSNR with the proposed Polar code
1.	Cameramn	33.3309	5.2115	12.7689	31.052
2.	Lena	39.1142	6.5210	16.2311	39.289
3.	Barbara	33.0623	11.1831	16.1894	33.130
4.	Boats	32.7802	9.3186	9.0565	32.634
5.	Peppers.	40.0012	7.4273	15.0288	36.389

Table 2 compares the performance of different test images based on channel and without channel (both coded and uncoded cases). Also, it compares the performance of error-correcting code based on the convolution code and our proposed polar code. The performance of the different test images has different reconstructed image quality.

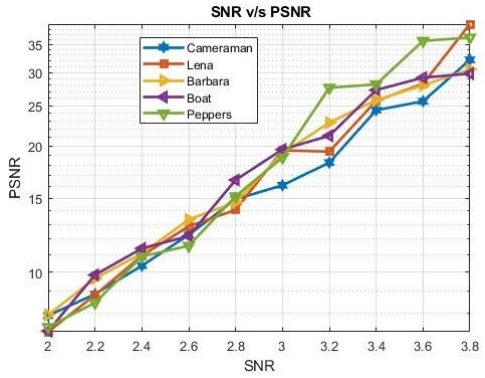

Fig. 10. PSNR performance comparison of different images over the multipath fading

The com-pressed sensing source coding method has been implemented without transmitting over a channel and that performance has been compared against the scenario when the image data is transmitted over a channel with OFDM modulation.

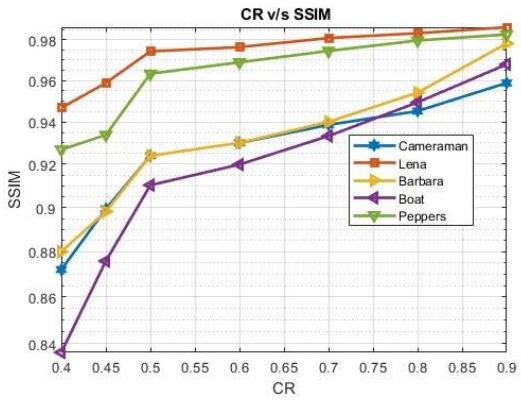

Fig. 11. Effect of compressive ratio on SSIM performance over the multipath fading channel

When it is passed through the multipath fading channel at signal to noise ratio of 5 dB without any error correcting code it is concluded that is then we found the worst result of the reconstructed image shown in Table 2. After that, we applied the convolution error correcting but we got a little better performance with this code. And when we used our proposed error-correcting code we got the best quality of the reconstructed image at low SNR=5dB. The visual inspection of the quality of the reconstructed images can be used to understand more clearly the effect of changing the SNR on the PSNR measurement metric, by taking the example of the image 'Peppers'. It can be seen that the reconstruction algorithm's performance worsens with lower SNR as can be logically concluded. We can visually perceive the effect a bad channel has on the communication of an image, with both the channel error control decoding and the reconstruction algorithm applied losing more information with worsening channel conditions. We can see that we can get a decent PSNR value of 33.97 and a well-reconstructed image at just a low SNR at just (3.5-4 dB).

TABLE 3

PNSR VALUE FOR A RANGE OF SNR VALUES AND POLAR CODES (1024, 512) FOR THE PEPPERS IMAGE

Method	SNR (dB)	0	0.4	0.8	1.2	1.6	2
Compressed image transmission with polar code (Proposed)	PSNR (dB)	16.7889	30.6711	36.3809	40.3436	40.3436	40.3436
Image transmission with polar code[Ref.12]	PSNR (dB)	7.90	8.42	10.05	13.23	17.48	22.30

Tables 3 and 4 are utilized to compare the reconstructed image quality of a test image, measured through PSNR.These tables allow for an assessment of performance based on varying *Signal-to-Noise Ratio* (SNR) levels and polar codes. By examining the data in these tables, it's possible to identify the combination of SNR and polar code that yields the highest image quality, thus determining superior performance compared to a provided reference standard. Figure 14 demonstrates the performance of the applied scheme of implementing polar code for a multipath fading channel with compressed sensing used for source coding. This simulation shows the performance of the applied model when the candidate image is changed. The compression ratio is fixed at 0.75, along with the code rate being fixed at 0.5. The number of significant signals paths (channel taps) is considered to be 3. The inference can be drawn from the above figure that the image over which the scheme is applied has no evident effect on the BER performance metric. This is intuitive as the nature of the source data should not affect the bit-error rate as that is only dependent on the channel coding and modulation models implemented. This is however not true for the PSNR metric of source coding (compressive- sensing) scheme applied, as has been observed before. We can see the impressive performance of the scheme of applying polar codes along with channel transformation.

TABLE 4

PNSR VALUE FOR A RANGE OF SNR VALUES AND POLAR CODES (1024, 512) FOR THE LENA IMAGE

Method	SNR (dB)	0	0.4	0.8	1.2	1.6	2
Compressed image transmission with polar code (Proposed)	PSNR (dB)	15.79	37.11	39.11	39.11	39.11	39.11
Image transmission with polar code [Ref.12]	PSNR (dB)	9.50	10.34	11.22	14.72	18.84	23.02

Bit-error rates of 10-5 can be achieved at signal-to-noise ratio in the range (3.5-4). This can be extrapolated from the slope of the curve so that we can achieve BER of the order of 10-9 for SNR in the range (4.5-5 dB). In Table 5, the performance of reconstructed images using a combination of Compressed Sensing (CS) and polar codes over a fading communication channel is evaluated. The *signal-to-noise ratio* (SNR) for this evaluation is set at 3.8 dB, and the *compression ratio* (CR) is 0.75. The results indicate that using polar codes in conjunction with Compressed Sensing improves the performance of the system compared to not using polar codes. Among the reconstructed images, the one corresponding to the "peppers" image achieved the highest Peak signal-to-noise ratio (PSNR) value of 40.3324 dB This PSNR value is indicative of high image quality and fidelity. The Structural Similarity Index (SSIM) value for the same "peppers" image is reported as 0.9811. SSIM values closer to 1 indicate that the reconstructed image closely resembles the original image in terms of structural details, contrast, and texture. These results suggest that when using Compressed Sensing with polar codes over a fading channel, the "peppers" image reconstruction stands out as having the highest image quality, as evidenced by its high PSNR and SSIM values. This demonstrates the effectiveness of polar codes in enhancing the reliability of the communication system and the quality of the reconstructed images. This study suggests that using polar codes in conjunction with compressed sensing improves the quality and reliability of reconstructed images over a fading communication channel, as evidenced by the higher PSNR and SSIM values, along with lower BER values. Figure 13 presents the performance comparison of using polar codes in conjunction with compressed sensing data over a multipath fading channel. In this evaluation, the performance of the system with polar codes is compared to the performance without polar codes.

The main result from Fig. 13 is that using polar codes significantly improves system performance in the context of compressed sensing over a multipath fading channel. This improvement can be attributed to the error-correction capabilities of polar codes, which effectively mitigate the adverse effects of signal fading, interference, and reflections associated with multipath channels.

TABLE 5

COMPARISON OF PSNR (dB), SSIM AND BER VALUES FOR DIFFERENT RECONSTRUCTED IMAGES USING COMPRESSED SENSING WITH POLAR CODE OVER A FADING CHANNEL WITH SNR=3.8 AND CR=0.75.

Error Correction		Without polar code with CR=0.75			With polar code with CR=0.75		
Parameters		PSNR (dB)	SSIM	BER	PSNR (dB)	SSIM	BER
Test Images	Cameraman	27.2178	0.6952	0.0251	33.3205	0.9384	4.2385e-06
	Lena	24.4811	0.9245	0.5431e-06	39.1124	0.9796	8.4771e-07
	Peppers	27.9057	0.9492	6.2165e-06	40.3324	0.9811	2.2606e-06
	Barbara	33.0612	0.9430	4.7641e-04	35.1594	0.9586	4.52177e-06

The use of polar codes enhances the system ability to recover data accurately, making it more resilient to communication challenges. This is especially valuable in scenarios where maintaining data integrity and signal quality is crucial, such as wireless communications, image transmission, or any application that involves transmitting data over unreliable channels.

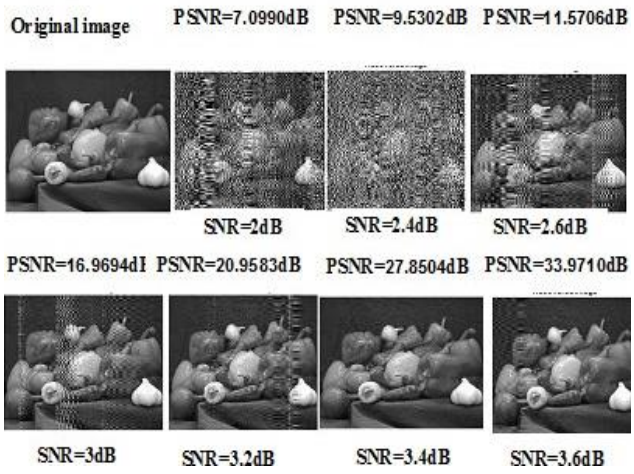

Fig. 12. Visual comparison of the reconstruction quality of the Peppers image for different SNR values

Figure 14 presents the *Bit Error Rate* (BER) performance of a communication system using polar codes in conjunction with compressed sensing data over a multi-path fading channel. It also offers a direct comparison between the BER performance when polar codes are employed and when they are not used in the context of compressed sensing over the same multi-path fading channel. The primary outcome depicted in Figure 14 is that utilizing polar codes leads to a substantial improvement in BER performance. Specifically, the BER is significantly lower when polar codes are integrated into the system compared to scenarios where polar codes are not utilized. Signifies that data transmission is more accurate and reliable. The multi-path fading channel introduces signal variations, making data transmission challenging due to interference and signal reflections. However, the presence of polar codes enhances the system's resilience in this challenging environment, resulting in fewer bit errors and more precise data recovery. This result has significant practical implications, particularly in wireless communication systems, where reliable data transmission is critical. It demonstrates that by employing polar codes in combination with compressed sensing, a communication system can achieve superior performance in terms of error correction and data recovery, even when confronted with adverse conditions like multipath fading.

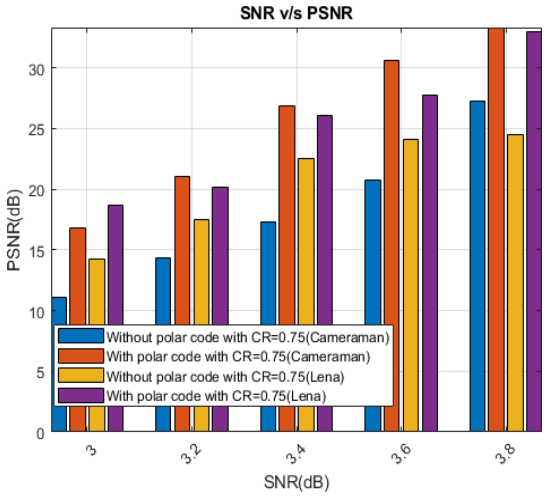

Fig. 13. PSNR performance comparison of different images over the multipath fading channel

In essence, Fig. 15 highlights the effectiveness of polar codes in enhancing the robustness and reliability of data transmission over multipath fading channels. The result provides insights about SSIM performance when employing polar codes in conjunction with compressed sensing data over a multi-path fading channel. Additionally, it offers a direct comparison of SSIM performance when polar codes are utilized versus when they are not employed in the context of compressed sensing over the same multi-path fading channel.

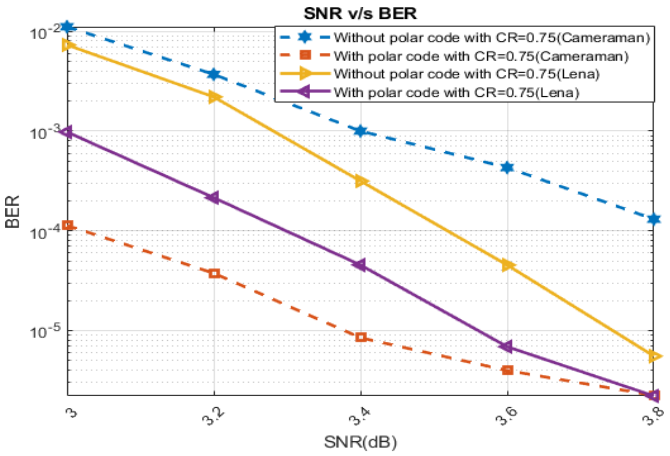

Fig. 14. BER performance comparison of different images over the multi-path fading channel.

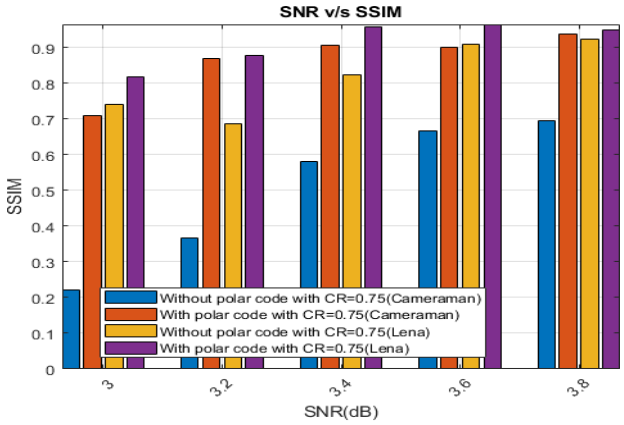

Fig.15. SSIM performance comparison of different images over the multipath fading channel

The key finding from Fig. 15 is that the use of polar codes yields significantly better SSIM performance. SSIM is a metric that measures the structural similarity between the original and reconstructed images, with a value of 1 indicating perfect similarity. In practical terms, the enhanced SSIM performance demonstrates that polar codes are effective in improving the quality of reconstructed images in the presence of multi-path fading. Multi-path fading introduces challenges such as signal degradation and interference, which can lead to distortions in images during transmission. However, the incorporation of polar codes helps mitigate these challenges, resulting in images that closely resemble their originals. This result has significance in applications where maintaining the integrity and quality of images or data is critical, such as medical imaging, video transmission, or remote sensing. By utilizing polar codes in combination with compressed sensing, the system can achieve better image fidelity and structural similarity, even under adverse conditions like multi-path fading. In summary, Figure 15 underscores the effectiveness of polar codes in enhancing the quality of reconstructed images in the context of compressed sensing over multi-path fading channels.

V. Conclusions

In this paper, we have proposed an efficient model based on compressive sensing, OFDM, and polar code with successive cancellation decoding to communicate the compressed data through wireless networks. A performance evaluation has been conducted for the proposed model over the multi-path fading channels. It is evaluated by communicating the compressed data using BPSK modulation over OFDM system with polar codes. A performance comparison of polar code with normal convolutional code has been also presented in the paper under the same scenario. The investigated results show that the performance of the polar codes is superior to the performance of convolutional codes in terms of the visual quality of received images and the bit error rate. In this paper, we have also laid out a detailed justification of our proposed model. The graphical analysis shows that compressed sensing signal communication with polar codes is an excellent candidate for reliable and efficient communication of the compressed data in wireless networks over the multipath fading channel at very low SNR=3.6dB. It is concluded that comparatively compressive sensing based on polar codes is a good selection for wireless image communication.

Acknowledgments

This work was sponsored by IDEAS, Technology Innovation Hub@ Indian Statistical Institute under Development of Data Science method for Cyber Physical system, DRIE/RDC/NM-ICPS/ISI Kolkata/2022-23/9483.

References

[1] F. C. Abdennour, B. A. Riad and R. Mehdi, “High-Capacity Transmission with Dual Polarization M-QAM Levels Based on DWDM Technique for Wireless Networks.” in *Microwave Review*, vol. 29, no. 1, 2023, ISSN 2406-1050

[2] B. Anes, B. A. Riad, “Filterless Photonic Millimeter Wave Generation and Data Transmission for 5G Indoor Wireless Access.” In *Microwave Review*, vol. 28, no. 1, 2022, ISSN 14505835

[3] T. Hemalatha and B. Roy, “A Comparative Study on Efficient MIMO Antennas in Wireless Communication,” in *Microwave Review* vol. 29, no. 1, 2023, ISSN 2406-1050

[4] E. J. Candes and M. B. Wakin, “An Introduction to Compressive Sampling,” in *IEEE Signal Processing Magazine*, vol. 25, no. 2, pp. 21-30, March 2008, DOI: 10.1109/MSP.2007.914731

[5] T. Arildsen, T. Larsen, “Compressed Sensing with a Linear Correlation Between Signal and Measurement Noise”, in *Signal Process*, vol. 98, 275–283, 2014, DOI: 10.1016/j.sigpro.2013.10.021

[6] M. Rani, S. B. Dhok, R. B. Deshmukh, “A Systematic Review of Compressive Sensing: Concepts, Implementations and Applications”, in *IEEE Access*, vol. 6, pp. 4875–4894, 2018, DOI: 10.1109/ACCESS.2018.2793851

[7] W. B. Pennebaker and J. L. Mitchell, *JPEG Still Image Data Compression Standard*, Kluwer Academic Publishers: Norwell, MA, USA, 1992.

[8] H. C. Huang and F.C. Chang, “Error Resilience for Compressed Sensing with Multiple Channel Transmission,” in *Journal of Information Hiding and Multimedia Signal Processing*, vol. 6, no. 5, pp. 847–856, Sep. 2015, ISSN 2073-4212

[9] E. Arikan, "Channel Polarization: A Method for Constructing Capacity-Achieving Codes for Symmetric Binary-Input Memoryless Channels," in *IEEE Trans. Information Theory*, vol. 55, no. 7, pp. 3051–3073, July 2009, DOI: 10.1109/TIT.2009.2021379

[10] H. Haneche, A. Ouahabi and B. Boudraa, "Compressed Sensing-Speech Coding Scheme for Mobile Communications," in *Circuits, Systems, and Signal Processing*, vol. 40, issue 10, pp. 5106-5126, 2021, DOI: 10.1007/s00034-021-01712-x

[11] F. Z. Moussa, F. Souheyla and Y. Belhadef, "New Design of Metamaterial Miniature Patch Antenna with DGS for 5G Mobile Communications," in *Microwave Review*, vol. 28, no. 2 2022, ISSN 2406-1050

[12] A. M. A. Garcia, M. Alcoforado, F. Madeiro and V. C. Rocha, "Improving Image Transmission by Using Polar Codes and Successive Cancellation List Decoding," in *Annals of Disaster Risk Sciences*: ADRS 3.1, 2020, DOI: 10.51381/ADRS.V3I1.41

[13] R. Gallager, "Low-Density Parity-Check Codes," in *IRE Transactions on Information Theory*, vol. 8, pp. 21-28, 1962, DOI: 10.1109/TIT.1962.1057683

[14] A. Mishra, K. Sharma and A. De, "Quality Image Transmission Through AWGN Channel Using Polar Codes," in *International Journal of Computer Science and Telecommunications*, vol. 5.1, pp. 8-16, 2014, ISSN 2047-3338

[15] H.-C. Huang, F.-C. Chang, T.-K. Huang, P.-L. Chen, "Error Control for Compressed Sensing Transmission with Polar Codes," *2019 IEEE 1st Global Conference on Life Sciences and Technologies (LifeTech)*, Osaka, Japan, 2019, DOI: 10.1109/LifeTech.2019.8883985

[16] G. L. Stüber, *Principles of Mobile Communication*, vol. 2, Boston: Kluwer Academic, 2001.

[17] H. Haneche, B. Boudraa and A. Ouahabi, "Compressed Sensing Investigation in an End-To-End Rayleigh Communication System: Speech Compression," *2018 International Conference on Smart Communications in Network Technologies (SaCoNeT)*, 2018, DOI: 10.1109/SaCoNeT.2018.8585702

[18] H. Haneche, B. Boudraa and A. Ouahabi. "A New Way to Enhance Speech Signal Based on Compressed Sensing," in *Measurement*, vol. 151, p. 107117, 2020, DOI: 10.1016/j.measurement.2019.107117.

[19] H. Haneche, A. Ouahabi and B. Boudraa, "New Mobile Communication System Design for Rayleigh Environments Based on Compressed Sensing-Source Coding", in *IET Communications*, 2019, DOI: 10.1049/ iet-com.2018.5348

[20] M. K. M. Al-Azawi and A. M. Gaze. "Combined Speech Compression and Encryption Using Chaotic Compressive Sensing with Large Key Size," in *IET Signal Processing* vol. 12. pp. 214-218, 2018, DOI: 10.1049/iet-spr.2016.0708

[21] Y. Ji, W.-P. Zhu and B. Champagne, "Recurrent Neural Network-Based Dictionary Learning for Compressive Speech Sensing," in *Circuits, Systems, and Signal Processing*, vol. 38, pp. 3616-3643, 2019, DOI: 10.1007/s00034-019-01058-5

[22] R. Mori and T. Tanaka, "Non-Binary Polar Codes Using Reed-Solomon Codes and Algebraic Geometry Codes," *2010 IEEE Information Theory Workshop*, Dublin, Ireland, 2010, pp. DOI: 10.1109/CIG.2010.5592755

[23] A. Hadi, *Optimization and Analysis of Polar Codes in Communication Systems*, Doctoral Thesis, Faculty of Science and Engineering, The University of Manchester, United Kingdom, 2018.

[24] H. Gan, S. Xiao, Y Zhao, X. Xue, "Construction of Efficient and Structural Chaotic Sensing Matrix for Compressive Sensing," in *Signal Processing: Image Communication*, vol. 68, pp. 129-137, 2018, DOI: 10.1016/j.image.2018.06.004

[25] X. Wang and Y. Su, "Image Encryption Based on Compressed Sensing and DNA Encoding." in *Signal Processing: Image Communication*, vol. 95, p. 116246, 2021, DOI: 10.1016/j.image.2021.116246

[26] T. N. Canh, Thuong and B. Jeon, "Restricted Structural Random Matrix for Compressive Sensing," in *Signal Processing: Image Communication*, vol. 90, p. 116017, 2021, DOI: 10.1016/j.image.2020.116017

[27] G. Javadi, A. Hajshirmohammadi and J. Liang, "Power and Sub-Channel Optimization of JPEG 2000 Image Transmission Over OFDM Based Cognitive Radio Networks," in *Signal Processing: Image Communication*, vol. 58, pp. 157-164, DOI: 10.1016/j.image.2017.08.002

[28] X. Li, X. Wan, M. Yang, J. Xue, N. Zeng, "A New Compressive Sensing Video Coding Framework Based on Gaussian Mixture Model," in *Signal Processing: Image Communication*, vol. 55, pp. 66-79, 2017, DOI:10.1016/j.image.2017.03.009